



University of Nevada, Reno



**Nevada Bureau of Mines and Geology Report 55**

# **Geothermal Resource Potential Assessment White Pine County, Nevada**



**Nicholas H. Hinz, Mark F. Coolbaugh, and James E. Faulds**

# **Nevada Bureau of Mines and Geology Report 55**

## **Geothermal Resource Potential Assessment, White Pine County, Nevada**

**Nicholas H. Hinz,  
Mark F. Coolbaugh, and  
James E. Faulds**

**Nevada Bureau of Mines and Geology  
University of Nevada, Reno**

**2015**



*Cover photo: Williams hot springs. Photo by Jim Faulds, 2012.*

# TABLE OF CONTENTS

Abstract.....	2
Potential Geothermal Resources .....	2
Known Conventional Fault-Controlled Geothermal Systems.....	2
Potential Unknown Blind, Conventional, and Fault-Controlled Geothermal Systems ....	8
Potential Deep Stratigraphic Reservoirs .....	13
Infrastructure Requirements.....	14
Environmental and Cultural Considerations/Impacts.....	18
Representative Project Description/Scenario .....	19
Acknowledgments .....	19
References.....	19

# ABSTRACT

Geothermal resources can potentially contribute toward the renewable energy portfolio of White Pine County (WPC) in two ways: first through the direct conversion of heat energy into electricity, and the second by way of direct-use applications in which thermal energy is used as a source of heat for buildings, greenhouses, and related structures. Several known geothermal areas within WPC lie proximal to the Southwest Intertie power line currently under construction.

A potential source of electricity could come from conventional geothermal systems associated with young faults and regions of active crustal deformation. These systems have a total installed capacity in the Great Basin region of nearly 1,000 MWe. White Pine County hosts several geothermal systems of this type, but none are currently producing electricity. White Pine County has relatively low rates of crustal deformation relative to western NV or the Wasatch region of Utah (e.g., faulting accommodating crustal extension). However, based on a review of the geology in the region, we conclude that sustained and reasonable exploration efforts could result in the discovery and development of one or more electricity-grade geothermal systems, with potential generation capacity at each system in the range of 1–20 MWe.

In addition, a new and unproven type of potential geothermal resource termed “deep stratigraphic reservoirs” or “hot sedimentary aquifers” has recently been proposed in the western United States. White Pine County, and in particular, the northern Steptoe Valley, has some of the most promising potential for electricity generation from this type of reservoir in the United States. Preliminary calculations suggest that as much as 500 MWe of baseload electricity in the northern Steptoe Valley could be produced from this type of reservoir using wells reaching depths of 2 to 4 km. The economic feasibility remains unproven, but initial estimates are encouraging.

Based on observed surface temperatures and flow rates of springs, several geothermal systems in WPC also have the potential for direct use, including the heating of buildings and greenhouses. Such uses could reduce the consumption of electricity generated from fossil fuels and could lead to economic expansion by extending the growing season for certain agricultural products and reducing utility costs.

## POTENTIAL GEOTHERMAL RESOURCES

### KNOWN CONVENTIONAL FAULT-CONTROLLED GEOTHERMAL SYSTEMS

White Pine County (WPC) is located near the center of the Great Basin (figure 1), an area that hosts more than 400 known geothermal systems with temperatures ranging from 37 to 270°C (Faulds et al., 2012). Most of these geothermal systems are not related to upper crustal magmatic heat sources (e.g., Kennedy and Soest, 2007) but are instead structurally (fault) controlled. Temperatures are generally >200°C at 5 to 6 km depth across much of the Great Basin, whereas average temperature gradients range from 15 to 80°C/km in the upper 1 km of crust (SMU, 2011). The conventional structurally controlled geothermal systems in the Great Basin are associated with permeable fault zones that facilitate convective heat flow. Currently, there are 27 geothermal systems that have been developed and are producing electricity within the Great Basin region (Faulds et al., 2013, unpublished data). Excluding the four higher enthalpy magmatic systems (e.g. Coso, 215°C, 274 MWe) and the four lowest temperature systems (~105°C, 0.3–2.2 MWe each) that have been developed, the average producing, amagmatic (i.e., not related to volcanic or magmatic activity) geothermal system in the Great Basin region generates approximately 20 MWe from 140 to 250°C reservoirs at <1 to 2 km depth. A new power plant that began test runs in 2014 near Paisley, Oregon, is expected to produce about 3 MWe from a 115–120°C reservoir (Crawford, 2013) and is a good example of what can be achieved in the 110–120°C temperature range throughout the Great Basin region. At slightly higher temperatures, the Don A. Campbell geothermal resource produces 19 MWe (net) from a 129°C reservoir (Orenstein and Delwiche, 2014).

Evaluation of publically available geothermal databases (NBMG and GBCGE, 2012; SMU, 2008) has identified six areas with shallow thermal groundwater in WPC (table 1, figure 2), with temperatures in springs and wells ranging from 23 to 88°C. Of greatest interest for possible direct or indirect energy utilization are three geothermal systems, located at Monte Neva Hot Springs, Cherry Creek Hot Springs, and Williams hot springs (figure 3), which have surface or near-surface temperatures of 88, 87, and 53°C, respectively. Geothermal water at each of these areas has a strong bicarbonate/carbonate signature (figure 4), which in many parts of the world indicates relatively low to moderate temperatures at depth (up to 120°C). However, the eastern Great Basin, including WPC, has thick sequences of carbonate rocks (limestone and dolomite), and in such terrains, thermal fluids could have relatively high temperatures at depth in spite of the strong bicarbonate/carbonate fluid signature. Two examples of electricity-producing geothermal systems with bicarbonate fluid signatures and subsurface temperatures approaching or exceeding 200°C are Beowawe, Nevada (White, 1963, 1968; Mariner et al., 1983), and Kizildere, Turkey (Dominco and Samilgil, 1970; figure 4).



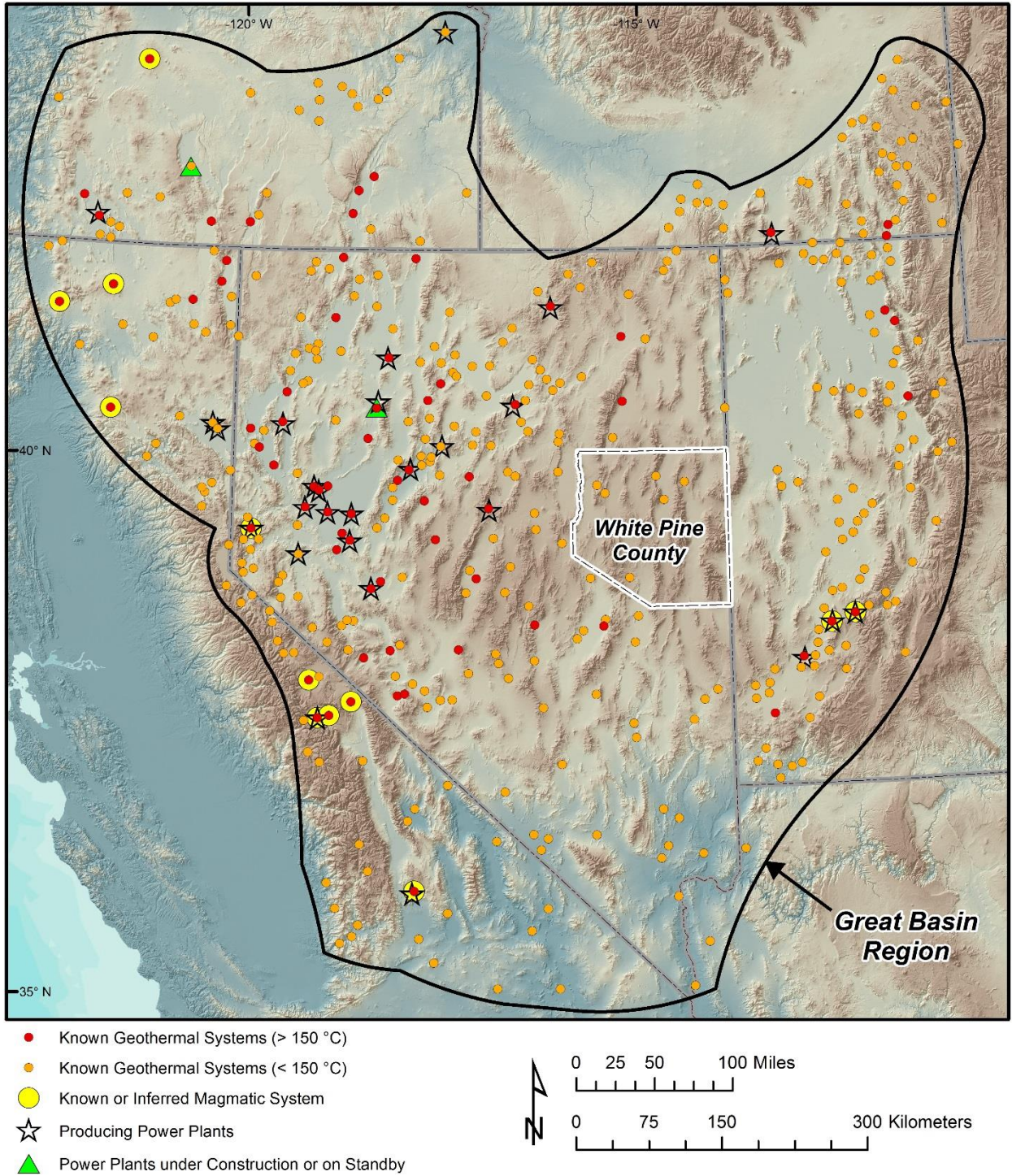


**Figure 1.** Geothermal systems and geothermal power plants in the Great Basin region. In this figure, symbols for power plants and magmatic systems sit underneath the red and orange symbols for geothermal systems > 150° C and < 150° C, respectively. Temperatures are based on the maximum of either the measured temperature or calculated temperature from geothermometry.

**Table 1.** Measured temperature and geothermometry of known geothermal systems in White Pine County (figure 2).

GIS Id	Geothermal System	Structural Setting	Maximum Measured Temperature (°C)	Geothermometry (°C)
1	Williams hot springs	Accommodation Zone	53 <sup>2</sup>	90-123 <sup>1,3</sup>
2	Monte Neva Hot Springs	Step-over	88 <sup>2</sup>	59-65 <sup>1,3</sup>
3	Cherry Creek Hot Springs	Step-over	87 <sup>2</sup>	99-109 <sup>1,3</sup>
4	Spring Valley well	Fault Intersection	32 <sup>3</sup>	79 <sup>3</sup>
5	Alligator Ridge well	Fault Intersection	34 <sup>3</sup>	44 <sup>3</sup>
6	Warm Springs Ranch	Step-over	23 <sup>3</sup>	42 <sup>3</sup>

<sup>1</sup>The range of “average” geothermometry calculated using two methodologies: 1) the method of Reed and Mariner (2007), involving silica and K-Mg geothermometers, and 2) the average of silica and Mg-corrected K-Na-Ca geothermometers using the choice of silica geothermometer based on the procedure of (Mariner et al., 1983).

<sup>2</sup>Temperatures from Garside and Schilling (1979).

<sup>3</sup>Temperatures and geothermometry from NBMG and GBCGE (2012).

Geothermometry can be used to estimate the temperatures of underlying fluid reservoirs beneath surface springs. This is important in geothermal energy development, because the higher the subsurface fluid temperature, the greater the potential for producing renewable energy. Geothermometry involves the prediction of subsurface temperatures based on the concentration of certain dissolved constituents in thermal waters, such as silica, sodium, and potassium. For example, higher concentrations of silica can be dissolved at higher temperatures, and similarly, the ratio of potassium to sodium increases as temperatures increase. When thermal fluids rise from depth toward the surface, they may cool significantly, but they commonly retain solute concentrations (e.g., silica, potassium, sodium) characteristic of their higher temperature history, because the chemical reactions that could cause re-equilibration at lower temperatures become sluggish or act slowly as temperatures decrease.

The silica, K-Mg, and Mg-corrected Na-K-Ca geothermometers of spring waters from Monte Neva, Cherry Creek, and Williams hot springs suggest relatively low to moderate subsurface geothermal reservoir temperatures, in the range of 59 to 123°C (table 1). Similarly, a ternary plot of Na, K, and Mg concentrations in hot spring waters (figure 5) predicts relatively low subsurface temperatures utilizing the Na-K and K-Mg geothermometers and methodology of Giggenbach (1988). For comparative purposes, it can be seen that the known high-temperature geothermal systems producing electricity at Beowawe, Nevada, and Kizildere, Turkey, have higher predicted subsurface temperatures than measured subsurface temperatures, as do thermal waters from the Marys River area of Elko County, Nevada (figure 5).

Although subsurface fluid temperatures predicted by geothermometry are moderate, they still indicate the potential for generating electricity where temperatures exceed 100°C. Geothermal power plants in the Great Basin with production brine temperatures near 100°C include Wabuska in western Nevada and Amedee and Wendel in eastern California. In such cases, power production is likely to be on the order of a few megawatts or less and require much higher flow rates than equivalent moderate or higher temperature systems.

Geothermometers are not always accurate predictors of subsurface fluid temperatures, because during their rise toward the surface, thermal fluids can precipitate minerals, re-equilibrate with surrounding rocks, or mix with shallow groundwater. Each of these mechanisms alters the original geochemical signature of the water, and in such circumstances, geothermometry may not accurately estimate temperatures at depth or give an indication of target depth for drilling. For example, Monte Neva Hot Springs, geothermometry predicts subsurface temperatures lower than that observed at the surface (table 1). The presence of relatively high Mg concentrations in Monte Neva spring water is an indication of possible mixing with shallower, cooler groundwater, which commonly is enriched in Mg. Such fluid mixing typically reduces the calculated temperatures of the more reliable geothermometers, including silica geothermometers, the Mg-corrected Na-K-Ca geothermometer, and the K-Mg geothermometer. The northern Steptoe Valley, where Monte Neva and Cherry Creek Hot Springs reside, is known to have relatively high temperatures at shallow depths based on deep drilling (see following section). Based on these temperatures and because the chemistry of waters at Monte Neva Hot Springs appears modified, it is possible that fluid reservoir temperatures beneath these springs are significantly hotter than predicted by geothermometry.



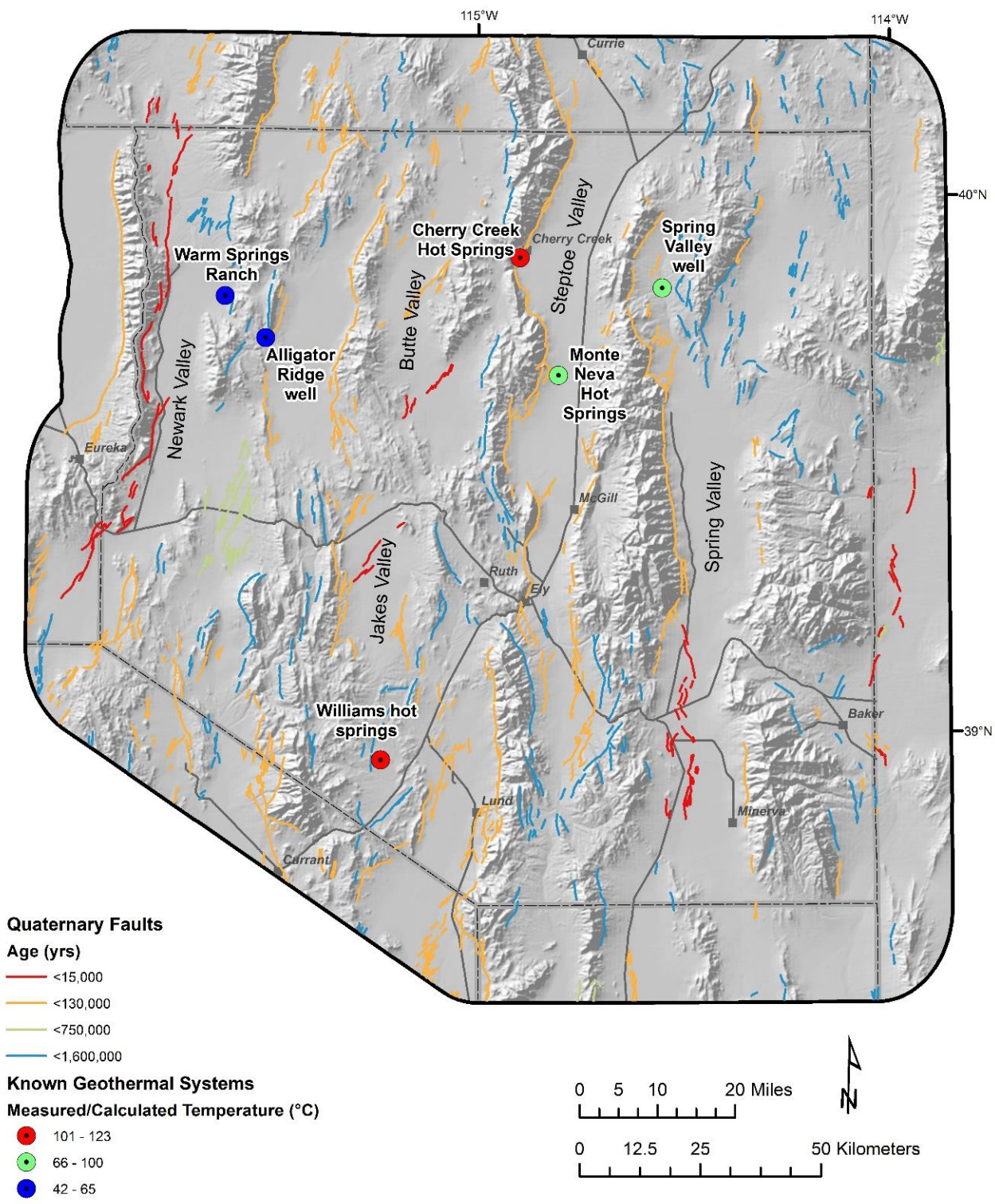


**Figure 2.** Shaded relief map of WPC showing known geothermal systems (table 1) and Quaternary faults (USGS and NBMG, 2006).





**Figure 3.** Williams hot springs overview. A) View is looking west at the east side of the White Pine Range in the background. B) One of the primary hot springs at Williams hot springs emanates into a broad ditch constructed for pipes to collect water for a concrete recreational soaking pool down slope. *Photos by Jim Faulds, 2012.*



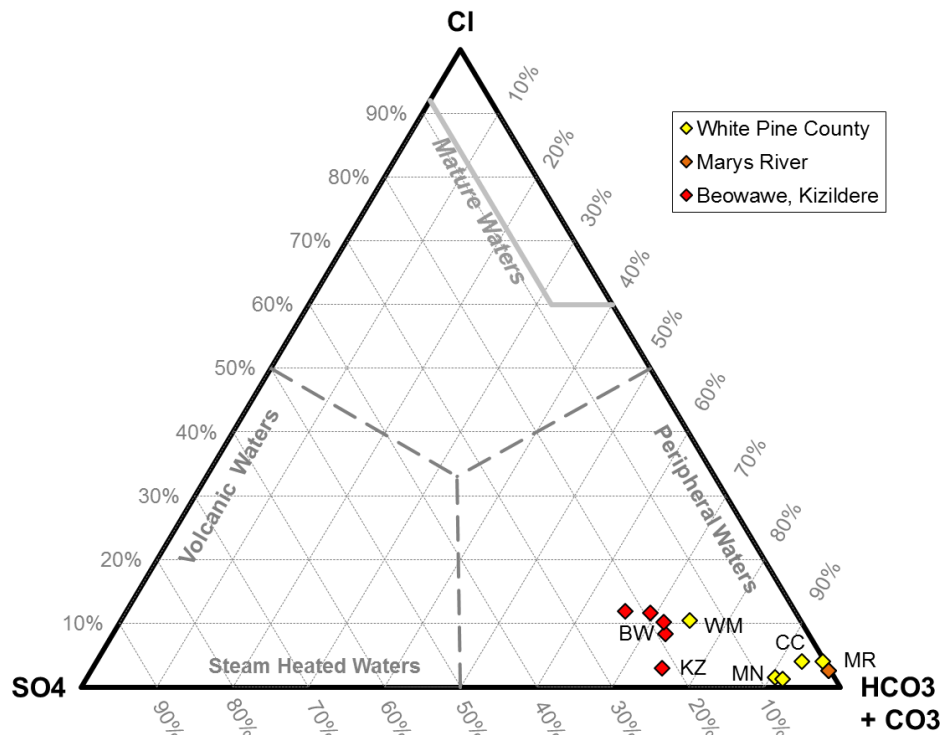


**Figure 4.** Ternary Cl-SO<sub>4</sub>-HCO<sub>3</sub> plot of ion proportions in hot spring fluids from WPC compared with Marys River (Elko County, NV), and producing systems in carbonates from Beowawe (Lander and Eureka counties, NV) and Kizildere, Turkey. BW = Beowawe, CC = Cherry Creek, KZ = Kizildere, MN = Monte Neva, MR = Marys River, WM = Williams hot springs.

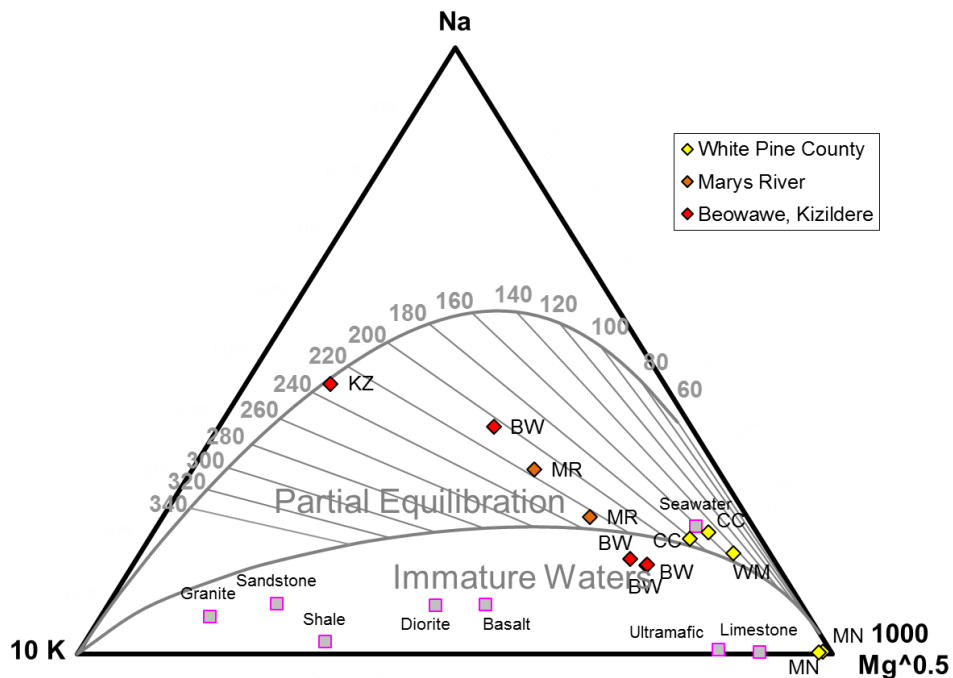


**Figure 5.** Na-K-Mg ternary geothermometer plot for hot spring fluids from WPC compared with Marys River (Elko County, NV), and producing systems in carbonates from Beowawe (Lander and Eureka counties, NV) and Kizildere, Turkey. See figure 4 caption site abbreviations. Higher subsurface temperatures are predicted for those samples that plot a greater distance from the Mg apex and closer to the K apex.

Research has shown that most of the known geothermal systems in the Great Basin region are associated with specific fault patterns or structural settings. The most common settings include terminations of major normal faults, accommodation zones (belts of intermeshing, oppositely dipping faults), step-overs in range-front faults, and fault intersections (Faulds et al., 2011, 2013). In contrast, the central segments of major normal faults with maximum displacement contain relatively few geothermal systems. Not every one of the favorable settings across the Great Basin region host geothermal systems, but they are a good place to prospect for blind, undiscovered geothermal systems (e.g., Kratt et al., 2010; Anderson and Faulds, 2013). The structural settings are defined for 5 of the 6 known geothermal areas in WPC (figure 2). Both Monte Neva Hot Springs and Cherry Creek Hot Springs are associated with step-overs in the range-front fault along the western side of Steptoe Valley. Warm Springs Ranch is associated with a combination step-over and fault intersection along the east side of Newark Valley, and the Alligator Ridge well is associated with a fault intersection at the south end of Alligator Ridge along the west side of Long Valley. Although a detailed analysis is needed, Williams hot springs may occupy an accommodation zone between oppositely dipping, Quaternary-active fault systems. There is insufficient geologic data available to characterize the structural controls of the Spring Valley well.

## **POTENTIAL UNKNOWN BLIND, CONVENTIONAL, AND FAULT-CONTROLLED GEOTHERMAL SYSTEMS**

Based on an evaluation of the Cenozoic extensional framework using geologic maps, publications, and fault databases (Stewart and Carlson, 1978; Stewart, 1998; USGS and NBMG, 2006), we have identified 48 favorable structural settings potentially capable of hosting geothermal activity in WPC (table 2, figures 6, 7). These favorable structural settings include fault step-overs, accommodation zones, fault bends along range-front faults, fault intersections, terminations of major normal faults, and compound settings with two or more overlapping structural settings. All of these structures are related to normal and/or transverse faults associated with Cenozoic extension. Four of the 48 structures in WPC are associated with known geothermal systems. There is minimal existing temperature and geochemical data in these areas to confirm or deny whether the remaining 44 structures host geothermal systems. The spatial density of known geothermal systems in eastern Nevada is overall lower than the density in northwest Nevada or central Utah (Faulds et al., 2012). However, it is not unreasonable to expect that one or more new structurally controlled economic resources could be found in WPC with the potential of producing 1–20 MWe per system.

To help prioritize the resource potential of the 44 favorable structural settings identified in this study, we have listed the age of faulting and analyzed the slip and dilation tendency of the primary faults defining each of these areas. The majority of the high-temperature systems ( $\geq 150^{\circ}\text{C}$ ) in the Great Basin region are associated with faults active in the Holocene (i.e., past ~12,000 years, Bell and Ramelli, 2007). Similarly, geodetically-derived strain rate models for the Great Basin positively correlate with the regional density distribution of both high- and low-temperature geothermal systems (Faulds et al., 2012). For this study, the age of faulting was derived from review of aerial photo imagery and the USGS Quaternary fault and fold database (USGS and NBMG, 2006).

Critically stressed fault strands are the most likely fault segments to act as fluid flow conduits (Barton et al., 1995; Sibson, 1994; Townend and Zoback, 2000). The tendency of a fault segment to slip or to dilate provides an indication of which sections of a fault zone within a geothermal system are most likely to transmit geothermal fluids (Morris et al., 1996; Ferrill, et al., 1999). Slip and dilation tendency values were obtained for each fault in the USGS Quaternary fault database (USGS and NBMG, 2006) within WPC. The USGS database does not include dip of these faults and because most of these faults are normal faults, a dip of  $70^{\circ}$  was applied across the entire dataset. For reference, a variation in  $\pm 10^{\circ}$  dip will not greatly affect the result of this analysis. The resultant slip and dilation tendency values are based on unitless ratios of the resolved stresses applied to the fault plane by the measured ambient stress field (e.g., Heidbach et al., 2008). Values range from a maximum of 1, a fault plane ideally oriented to slip or dilate under ambient stress conditions, to zero, a fault plane with no potential to slip or dilate. Slip and dilation tendency analyses were measured separately for each fault segment and then summed within a range of zero to 2.00 (figure 7). Each favorable structural setting includes multiple individual faults of differing orientations relative to the regional stress field and each with specific slip and dilation tendency values, and therefore a qualitative assessment of the overall slip and dilation tendency of each structure as a whole. With respect to Cenozoic structures not associated with Quaternary scarps, key fault orientations were compared with the results of Quaternary faults of similar orientation located nearby. The resulting slip and dilation tendency analysis scores for the favorable structural settings in WPC ranged from 0.30 up to 1.40. These scores were subdivided into even thirds of the range in scores whereby High = 1.40 to 1.05, Moderate = 1.04 to 0.68, and Low = 0.67 to 0.30 (table 2).



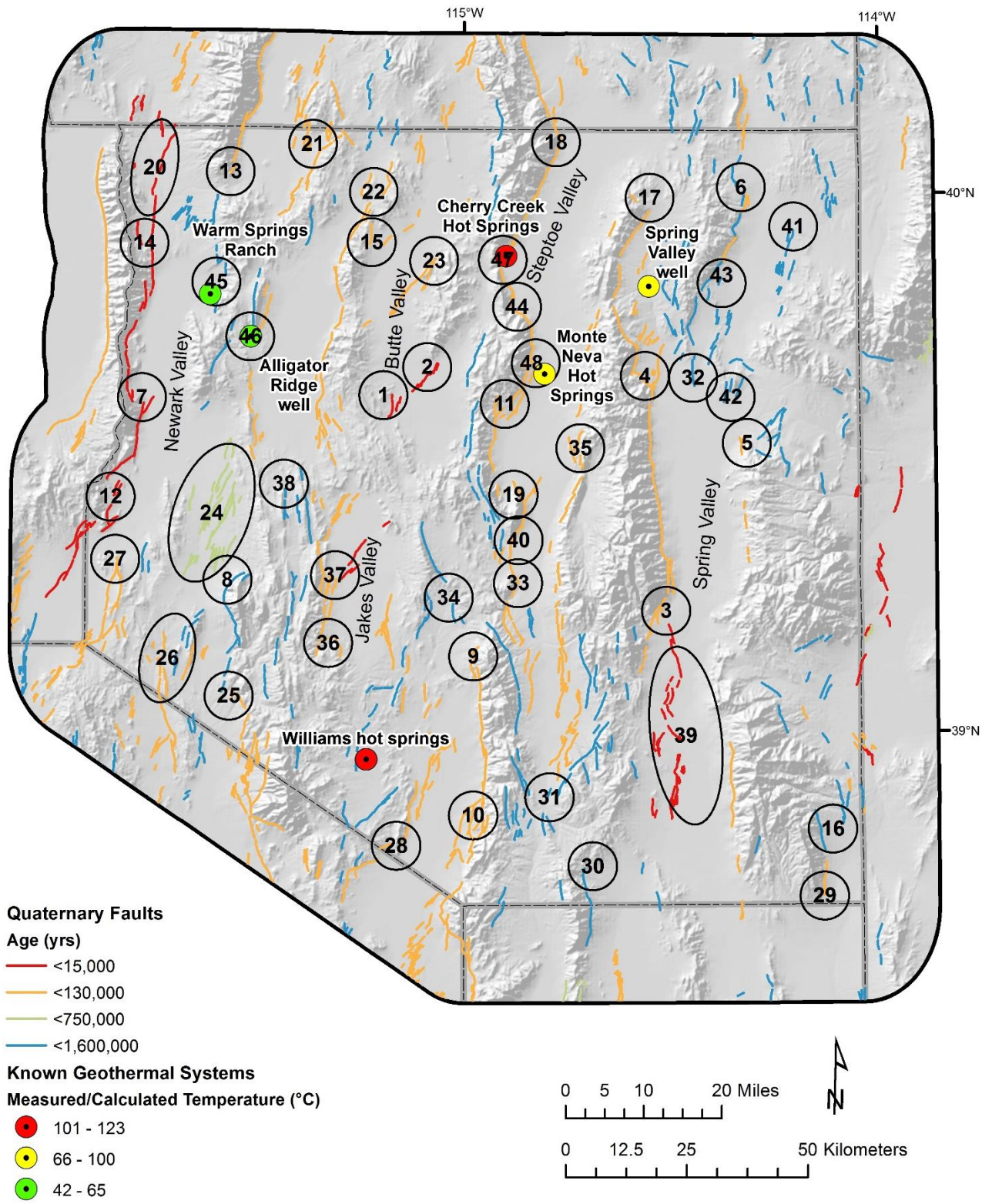


**Figure 6.** Shaded relief map of White Pine County showing known geothermal systems (table 1), age of Quaternary fault activity, and favorable structural settings that could host undiscovered blind geothermal systems (table 2). Favorable structural settings are depicted with a circle or oval that is larger than most well fields of producing systems (1–3 square miles; e.g., fig. 11). The size of the polygon depicts the general target area within which a resource may reside.



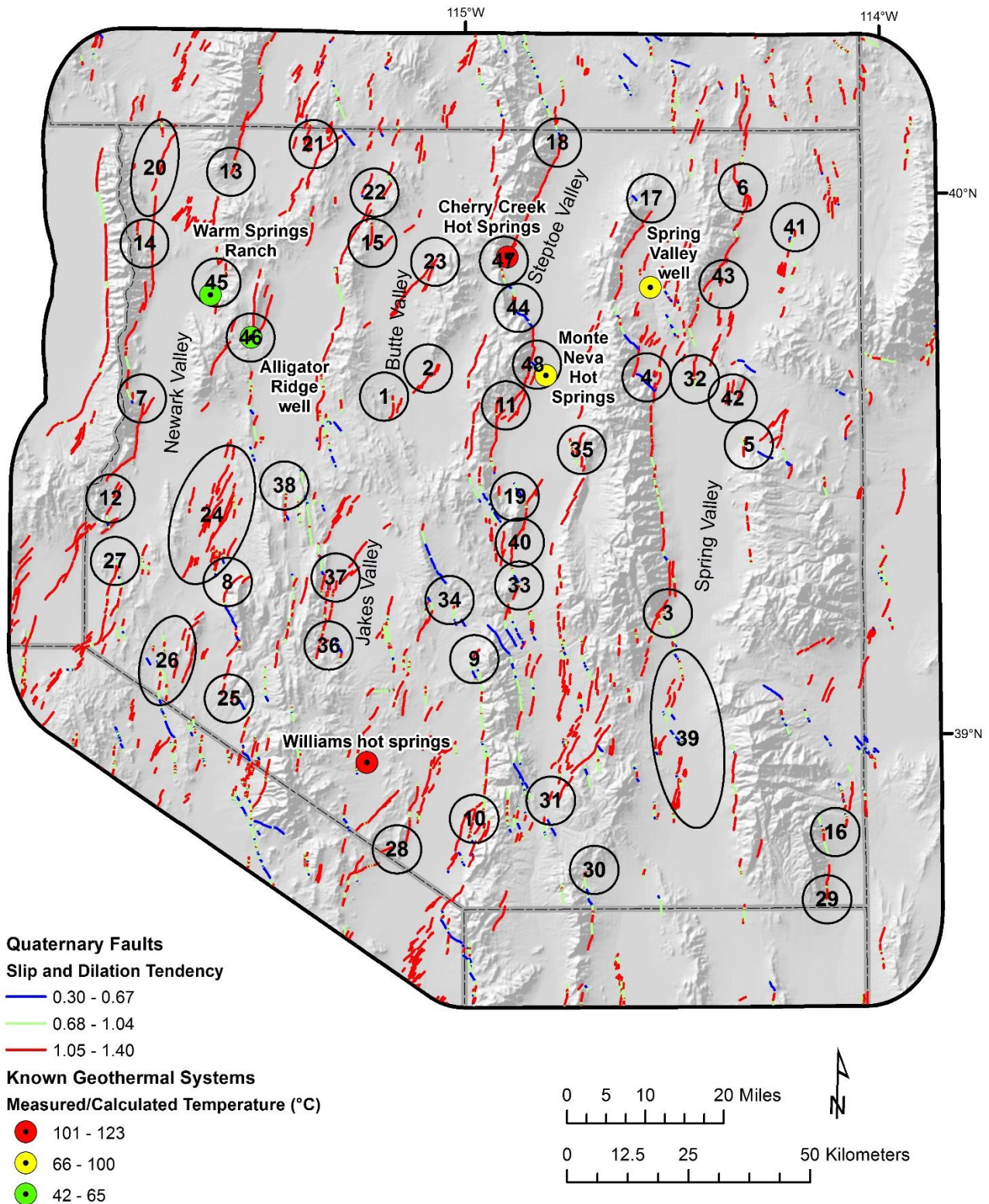


**Figure 7.** Shaded relief map of White Pine County showing known geothermal systems (table 1), the results of slip and dilation tendency analysis, and favorable structural settings that could host undiscovered blind geothermal systems (table 2). Favorable structural settings are depicted with a circle or oval that is larger than most well fields of producing systems (1–3 square miles; e.g., figure 10). The size of the polygon depicts the general target area within which a resource may reside.



**Table 2.** Favorable structural settings that may host undiscovered blind geothermal systems in White Pine County (figures 6, 7).

<b>GIS Id</b>	<b>Favorable Structural Setting</b>	<b>Age of faulting (yrs)</b>	<b>Slip and Dilation Tendency Rating</b>	<b>Description</b>
1	Accommodation Zone	<15,000	High	South end of synclinal accommodation zone between the east-tilted Butte Mountains and the west-tilted southern end of the Cherry Creek Range
2	Fault Termination	<15,000	High	Termination of primary range-front fault along the southeast side of the southern Cherry Creek Range terminates into Butte Valley
3	Step-over	<15,000	High	Step-over in range-front fault along the east side of the Schell Creek Range between Black Mountain and Cave Mountain
4	Step-over	<130,000	High	Step-over in range-front fault along the east side of the Schell Creek Range in the Frenchmen Creek and North Creek area
5	Fault Termination	<130,000	Moderate	Termination of range-front fault at the north end of the Snake Range
6	Step-over	<130,000	High	Step-over along the east side of the Antelope Range in the Cottonwood Canyon-Chin Creek area
7	Step-over	<15,000	High	Step-over along the east side of the Diamond Mountains/west side of Newark Valley, northeast of Diamond Peak
8	Fault Bend	<1,600,000	High	Broad fault bend in range-front along northwest end of the White Pine Range near Seligman and Mohawk Canyon
9	Fault Termination	<130,000	Moderate	Termination and possible fault bend of the range-front fault at the northwest end of the Egan Range
10	Step-over	<130,000	High	Step-over in the range-front fault along the west side of the Egan Range in the Lund area
11	Step-over	<130,000	High	Step-over in the range-front fault along the east side of the Egan Range in the Water Canyon and Dry Canyon area
12	Step-over	<15,000	High	Step-over along the southeastern end of the Diamond Mountains
13	Fault Termination	<130,000	High	Southern termination of range-front fault along the east side of the Ruby Mountains
14	Step-over	<15,000	High	Step-over along the east side of the Diamond Mountains northeast of Christina Peak in the Connors Creek area
15	Step-over	<130,000	High	Step-over along the east side of the Butte Mountains, west side of Butte Valley
16	Step-over	<1,600,000	Moderate	Step-over along the east side of the Snake Range between Chokeycherry Creek and Lexington Creek
17	Fault Termination	<130,000	High	Termination of the range-front fault along the northeast end of the Schell Creek Range in the Sampson Creek area
18	Fault Bend	<130,000	High	Fault bend along the range-front fault bounding the east side of the Cherry Creek Range in the Indian Creek area
19	Compound Fault Intersection and Step-over	<130,000	High	Fault intersection along the northeast side of Heusser Mountain in the Egan Range and a step-over along the east side of the Egan Range at "The Cove"
20	Accommodation Zone	<15,000	High	Synclinal accommodation zone between the east-tilted northern Diamond Mountains and the southern west-tilted Ruby Mountains
21	Step-over	<130,000	High	Step-over in range-front fault along the west side of Maverick Springs Range near the northern WPC boundary
22	Step-over	<130,000	High	Step-over along the west side of the Butte Mountains along Long Valley Wash
23	Fault Intersection	<130,000	High	Intersecting, oppositely dipping faults at the northeast end of Black Mountain, east side of the Cherry Creek Range
24	Accommodation Zone	<750,000	High	Anticlinal accommodation zone in southeastern Newark Valley between the northeast end of the Pancake Range and the northern White Pine Range

25	Step-over	<130,000	High	Step-over in the range-front fault zone along the west side of the White Pine Range in the Lampson Canyon and Freeland Canyon area
26	Accommodation Zone	<130,000	Moderate	Anticlinal accommodation zone between the Pancake Range and White Pine Range north-northwest of Railroad Valley
27	Fault Termination	<130,000	Moderate	Termination of range-front fault along the northwest side of the Pancake Range
28	Step-over	<130,000	High	Fault step-over along the west side of White River Valley, southeast of Lund
29	Fault Termination	<130,000	High	Fault termination along the southeast end of the Snake Range
30	Fault Termination	<1,600,000	Moderate	Fault termination along the west side of the Schell Creek Range northwest of Mount Grafton
31	Fault Termination	<1,600,000	High	Termination of range-front fault along the west side of the Schell Creek Range and termination of antithetic fault along the east side of the Egan Range at the south end of Steptoe Valley
32	Fault Termination	<1,600,000	Moderate	Termination of range-front fault at the south end of the Antelope Range at the north end of Spring Valley
33	Fault Bend	<130,000	Moderate	Prominent bend in the range-front along the east side of the Egan Range, directly north of Ely
34	Accommodation Zone	<1,600,000	Moderate	Synclinal accommodation zone northwest of Murry Summit in the Egan Range
35	Compound Fault Termination and Accommodation Zone	<130,000	High	Northward termination of range-front fault along the northwest end of the Duck Creek Range and a synclinal accommodation zone between the northern Duck Creek Range and the Schell Creek Range
36	Fault Termination	<130,000	High	Southward termination of range-front fault along the southwest corner of Jakes Valley, east side of the White Pine Range
37	Fault Intersection	<15,000	High	Fault intersection along the west side of Jakes Valley next to Moorman Ridge
38	Accommodation Zone	<1,600,000	Moderate	Accommodation zone between two southward-terminating faults bounding either side of Long Valley at the north end of the White Pine Range
39	Accommodation Zone	<15,000	High	Accommodation zone in Spring Valley between the Schell Creek Range and the southern Snake Range
40	Accommodation Zone	<130,000	High	Possible accommodation zone between Smith Valley and Steptoe Valley
41	Fault Termination	<1,600,000	Moderate	Northward termination of the fault zone in northeastern Antelope Valley, north of the South Mountains
42	Fault Termination	<1,600,000	High	Termination of normal fault along the southwest side of the Red Hills into the north end of Spring Valley
43	Fault Intersection	<1,600,000	High	Intersection between interbasinal fault in Antelope Valley near Red Rocks and the range-front fault along the southeast side of the Antelope Range
44	Step-over	<130,000	Moderate	Broad step-over along the east side of the Cocomongo Mountain extending from north end of the Egan Range to the Cherry Creek Range
45	Compound Step-over and Fault Intersection	<1,600,000	High	Combination step-over and fault intersection along the east side of Newark Valley
46	Fault Intersection	<130,000	High	Fault intersection at the sound end of Alligator Ridge along the west side of Long Valley
47	Step-over	<130,000	High	Step-over in the range-front fault along the western side of Steptoe Valley
48	Step-over	<130,000	High	Step-over in the range-front fault along the western side of Steptoe Valley



Nine of the 48 favorable structural settings are associated with faults active in the past 15,000 years and have faults with high slip and dilation tendency. These systems should be considered higher priority in exploration for undiscovered systems (highlighted in gray boxes in table 2). Exploration should be conducted in a systematic way using proven methodologies to first determine if a resource exists in one or more of these locations and then to vector in on the discrete productive zone (e.g., Coolbaugh et al., 2006; Kratt et al., 2010; Hinz et al., 2013).

The 48 favorable structural settings (or fault patterns) identified in this study are broadly distributed across WPC (figure 6), but the nine higher priority exploration targets are restricted to three parts of WPC. The three geographic areas with the higher priority favorable structural settings include 1) three fault step-overs and one accommodation zone along the west side of Newark Valley in the western part of WPC; 2) a fault termination and an accommodation zone in Butte Valley and a fault intersection Jakes Valley in the central part of WPC; and 3) a fault step-over and accommodation zone in southern Spring Valley in the southeastern part of WPC.

## POTENTIAL DEEP STRATIGRAPHIC RESERVOIRS

Many deep sedimentary basins throughout the world have hot water aquifers that cover very large extents. Development of such aquifers for electricity generation has generally not been feasible due to the moderate temperatures (<150°C), low permeability, and/or cost-prohibitive depths at which these reservoirs/aquifers commonly exist. However, recent documentation shows that in western Utah and eastern Nevada, these aquifers could have higher than typical temperatures of 175 to 200°C at potentially economically extractible depths of 3 to 4 km (Allis et al., 2011, 2012; Anderson, 2013; Deo et al., 2013). The existence of such aquifers at such depths is made possible by the relatively high heat flow and high temperature gradients in the western United States. Thick accumulations of sediments with low thermal conductivities in intermontane basins allow for high temperature gradients to develop where conductive heat flow is high (Allis et al., 2011, 2012, 2013). In eastern Nevada and western Utah, where heat flow reaches 80 to 100 mW/m<sup>2</sup>, temperatures can reach 175 to 200°C at depths of 3 to 4 km (figure 8).

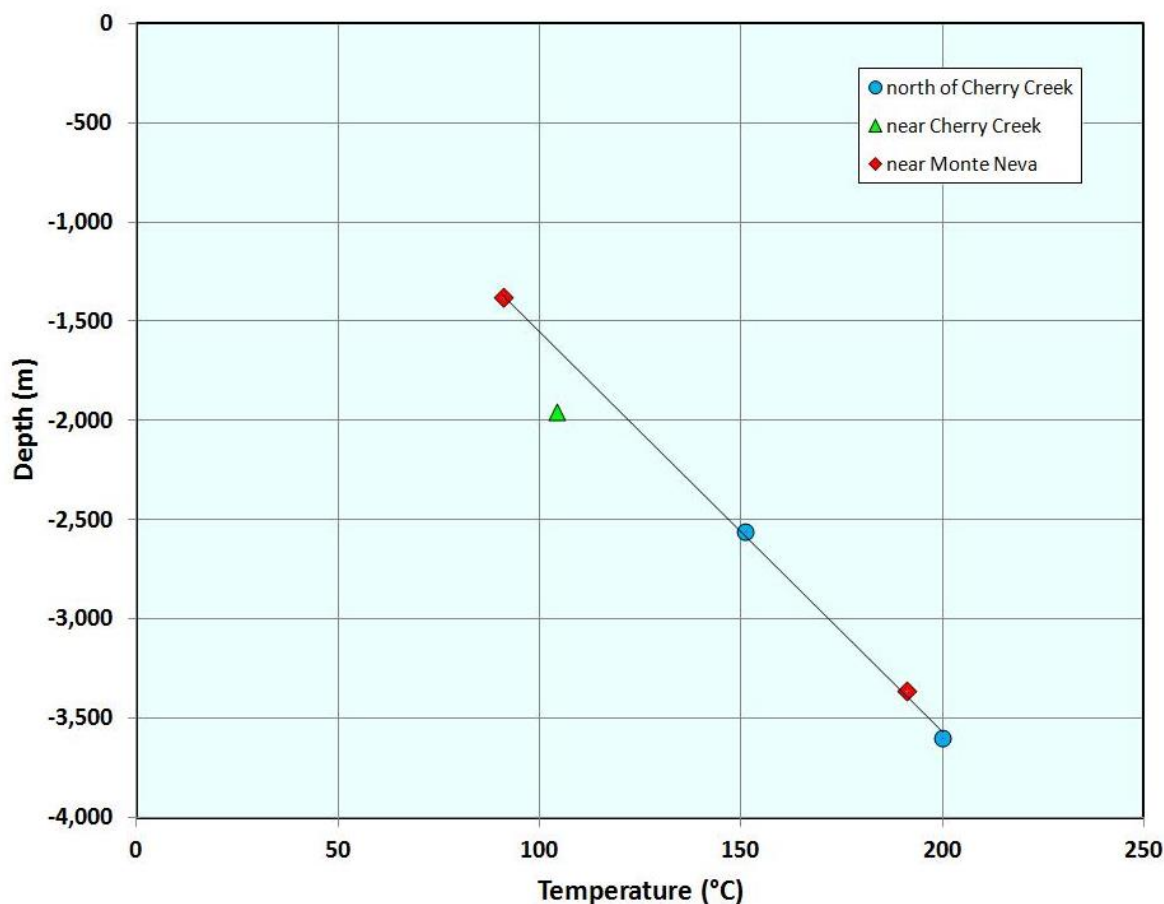


**Figure 8.** Graph showing relationship between depth and temperature in the northern Steptoe Valley. Potentially economic temperatures of 150 to 200°C exist at depths of 2.5 to 3.5 km below surface.

Data compiled from oil and gas drilling indicate that Lower Paleozoic carbonate rocks underlie basin fill in many valleys, and that these carbonates can have permeabilities necessary to sustain the flow rates needed for power production (Allis et al., 2012; Kirby, 2012). Based on available data, the most favorable valleys in the Great Basin for potential development of stratigraphic reservoirs are the Black Rock Desert in west-central Utah, the northern Steptoe Valley in WPC, Nevada, and the Marys River area of Elko County, Nevada (Allis et al., 2011, 2012). Preliminary modeling suggests that economic development of these deep aquifers is possible if sufficient permeabilities are present. The amount of produced power could range from 3 to 9 MWe/km<sup>2</sup> over a period of 30 years (Allis et al., 2013; Deo et al., 2013). In the case of the northern Steptoe Valley, where temperatures of 190 to 200°C at a depth of 3.5 km have been measured in oil exploration wells (figure 8), it is conceivable that as much as 500 MWe of electricity could be produced, assuming a power density of 4 MWe/km<sup>2</sup> (Allis et al., 2013; Deo et al., 2013) and an aquifer that covers 130 km<sup>2</sup>, which is the area defined by gravity modeling with basin fill depths of 2 km or more (e.g., Jachens, et al., 1996).

Available data indicate that in WPC, the northern Steptoe Valley provides the best environment for possible energy production from deep stratigraphic reservoirs. The Steptoe Valley has the highest upper crustal temperature gradient in WPC, based on temperature maps produced by Southern Methodist University (figure 9; Coolbaugh et al., 2005). Estimated depths of basin-fill deposits are also greatest for Steptoe Valley, based in part on modeling of regional gravity data (figure 9; Jachens et al., 1996). Direct measurements of temperatures in several oil exploration wells and deep geothermal exploration holes confirm temperatures of approximately 190 to 200°C at a depth of about 3.5 km (Allis et al., 2012; NBMG digital data). The area of principal interest extends northward in Steptoe Valley from Monte Neva Hot Springs approximately 25 to 30 km and corresponds to the region in figure 9, where the thickness of basin fill is predicted to exceed 2 km. In one well (Placid oil exploration well), a thick section of lost circulation was encountered at a depth of about 3 km, suggesting the possible presence of a significant thermal aquifer (Allis et al., 2012).

Although Steptoe Valley has the best documented potential for deep stratigraphic aquifer development, insufficient data are present to adequately evaluate the potential in many valleys of WPC. More detailed gravity, heat flow, and seismic reflection surveys would provide very helpful information for assessing this regional potential.

## INFRASTRUCTURE REQUIREMENTS

One of the key requirements for development of electrical energy from geothermal sources is the presence of suitable transmission lines. Fortunately, the location of the 500kV AC Southwest Intertie Project (SWIP) transmission line is well placed for access to potential geothermal resources in WPC (figure 10). The southern half of this line, which has just been constructed, passes over Williams hot springs, and the northern half of the SWIP will pass directly over the potential deep stratigraphic aquifer target in northern Steptoe Valley. The SWIP will also pass within a few miles of Monte Neva and Cherry Creek Hot Springs.

Typical local infrastructure associated with geothermal power beyond regional transmission line networks includes the power plant, service and access roads, a well field, and a connecting power line to the primary transmission lines (e.g., figure 10). With the exception of possibly using some existing roads and the regional transmission line network (figure 10), the rest of the infrastructure will need to be built for each geothermal area. The well fields include multiple graded well pads, service roads, and above-ground piping to carry geothermal fluids from the production wells to the power plant and then to the injection wells (figure 11). The layout and size of each of these infrastructure elements are custom designed for each geothermal area relative to the subsurface location of the productive reservoir, local topography, and potential local environmental and cultural considerations. Generally, the area impacted by exploration and development of a geothermal resource is nearly identical to that involved in the operation of the power plant except that some wells may be plugged and abandoned. Well fields for existing geothermal power plants in the Great Basin region utilize from one to six or more production wells and generally fewer injection wells. In some cases, multiple production wells may be achieved with vertical or deviated well paths from a single well pad. In addition to production and injection wells, monitor wells may also be used to monitor fluid flow within the reservoir.

Productive geothermal reservoirs are commonly not found directly underneath surface manifestations in the Great Basin region, but are rather found within <1 to 3 miles (<1 to 5 km) laterally of the surface manifestations (e.g., figure 11). The three conventional, structurally controlled geothermal areas in WPC with potential for power production all have active surface manifestations (hot springs). However, the reservoirs linked to these hot springs at depth have not been explored and thus the location of infrastructure necessary for exploration and development cannot be precisely constrained in this study.



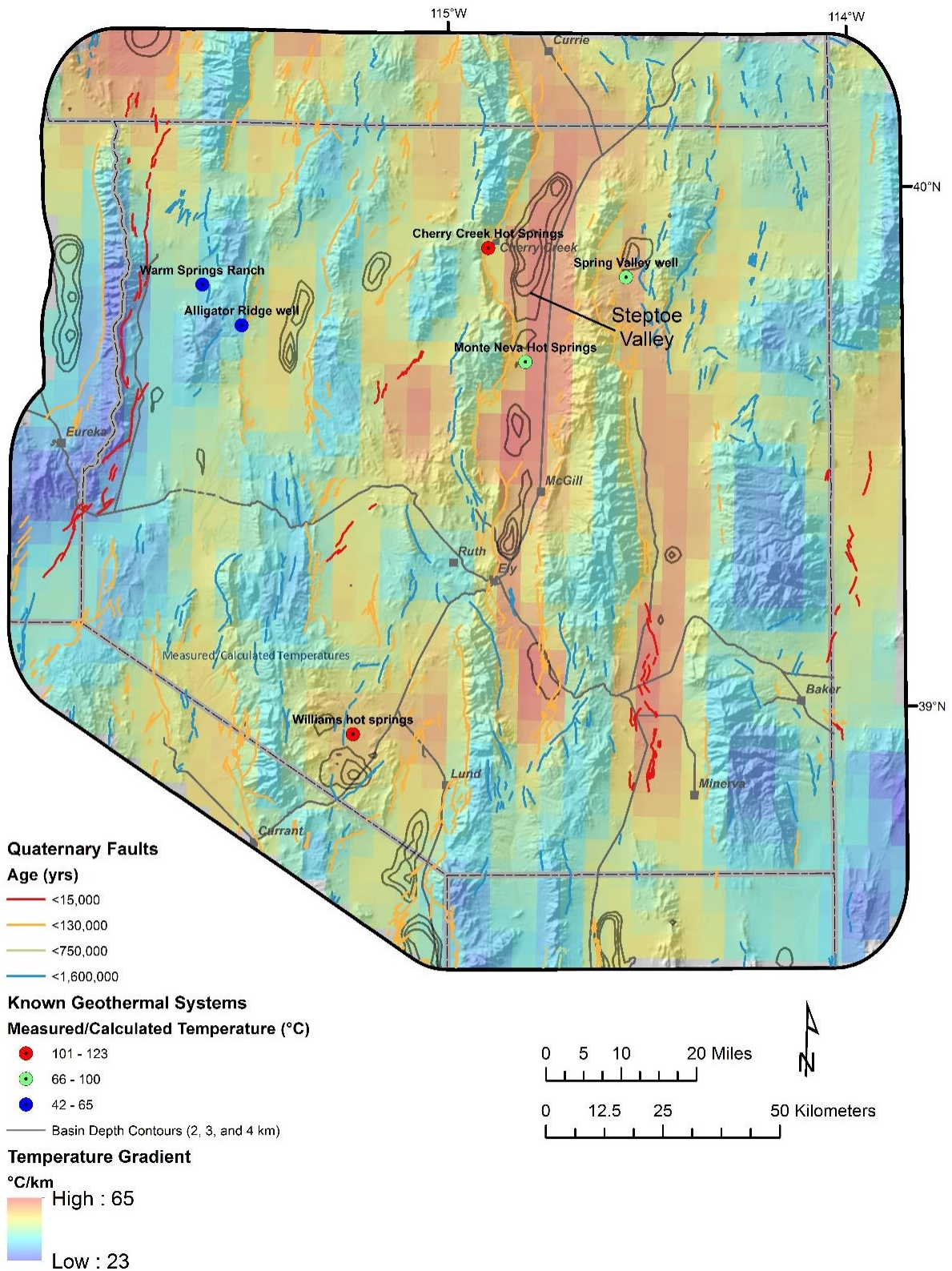


**Figure 9.** Shaded relief map of WPC with known geothermal systems (table 1) and Quaternary faults (USGS and NBMG, 2006). Upper crustal temperature gradient provided by Southern Methodist University (Coolbaugh et al., 2005). Black line contours represent estimated thickness of poorly consolidated late Cenozoic basin-fill sediments in 1 km intervals (black line contours) from Jachens et al. (1996).

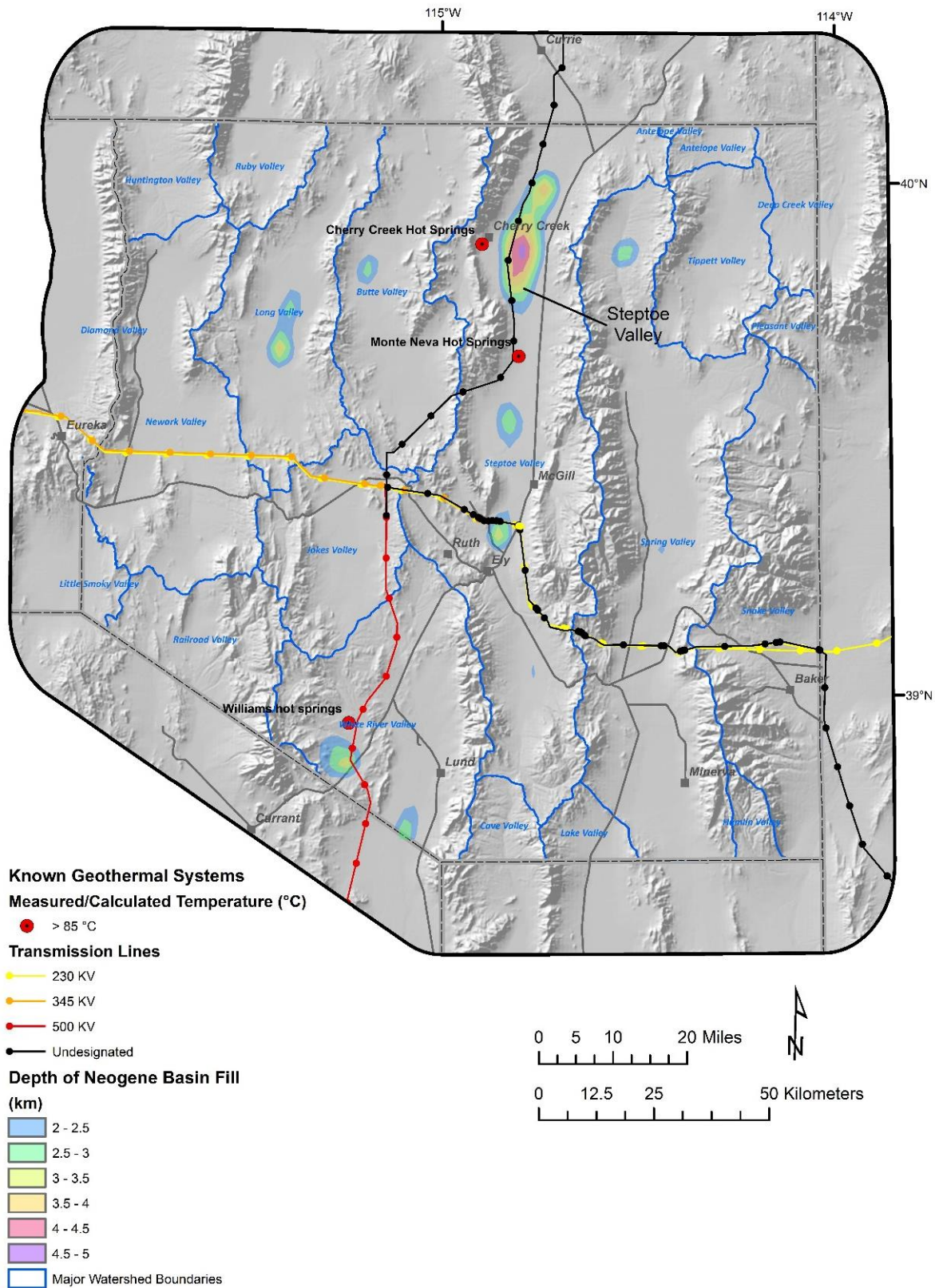


**Figure 10.** Map of transmission lines relative to the location of the principal geothermal resources in WPC and the best potential economic geothermal systems, including Williams hot springs, Monte Neva Hot Springs, Cherry Creek Hot Springs, as well as the deep sedimentary reservoir in Steptoe Valley.



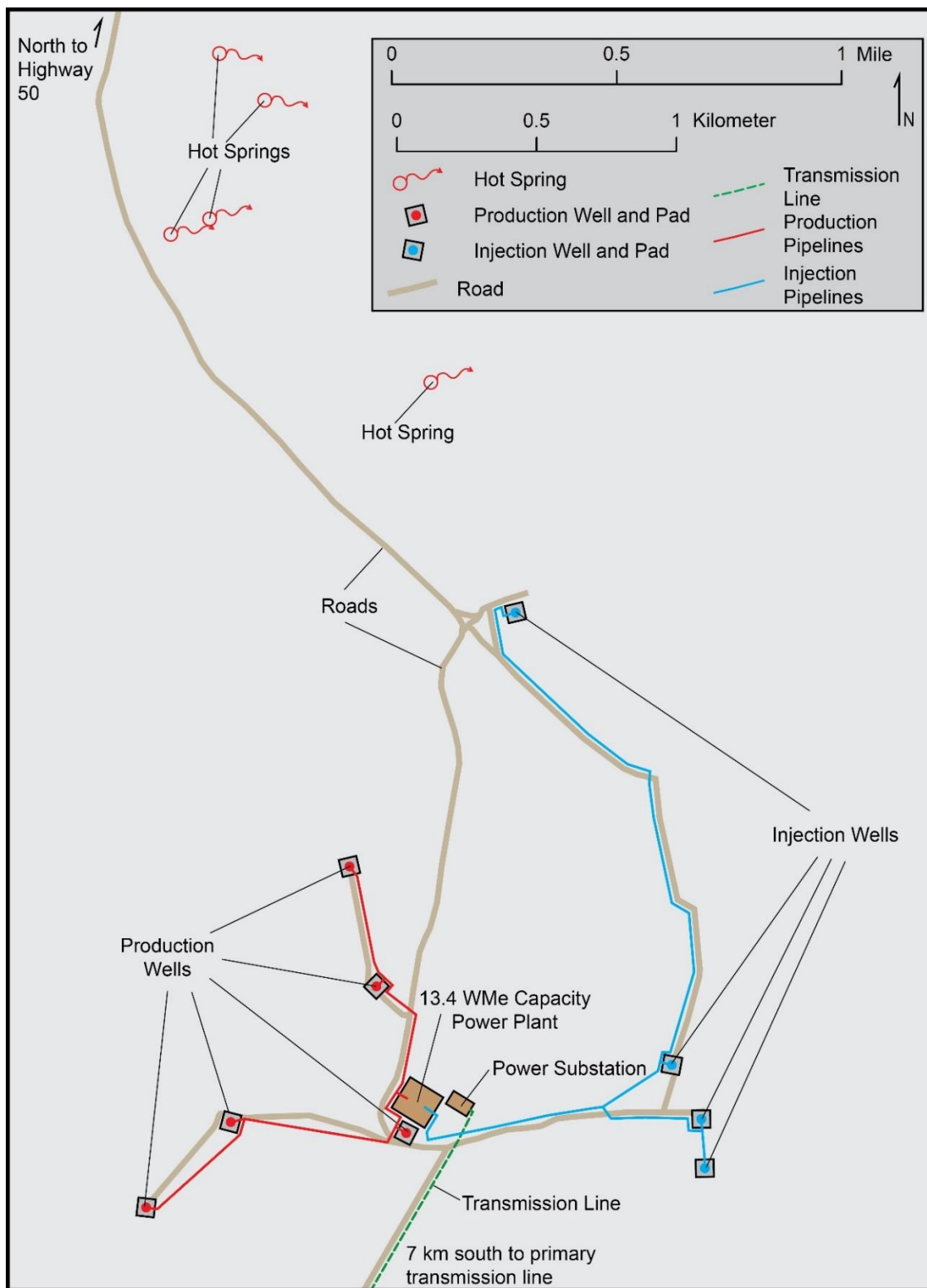


**Figure 11.** Generalized map showing primary infrastructure at the 13.4 MWe capacity Salt Wells geothermal power plant relative to active surface hot springs. Additional hot springs are present at the Salt Wells geothermal area to the north of this map area. The Salt Wells geothermal power plant resides in Churchill County, Nevada, is owned and operated by Enel Green Power North America, Inc., and has been in operation since 2009. This figure is a graphic illustration from a scaled map; generalized from Coolbaugh et al. (2006) and Hinz et al. (2011, 2014).



## ENVIRONMENTAL AND CULTURAL CONSIDERATIONS/IMPACTS

Geothermal power plants have exceptionally small footprints (figures 11, 12). In the case of binary power plants (e.g., figure 11), which are typically utilized for resources  $<200^{\circ}\text{C}$ , carbon emissions are near zero, and all fluids from production wells are re-injected into the ground through injection wells for recirculation. Minor to moderate amounts of *makeup* water may be needed for pressure maintenance and environmental considerations. Some plants also use water cooled towers which uses additional water.

Geothermal wells are cased in steel and cement, and the casings are only left open at productive reservoir depths. This design restricts inflow of cold water into the production wells and also restricts contamination of shallow aquifers otherwise not naturally connected with the deeper productive reservoir. In circumstances where a well is no longer needed, there are regulations for proper permanent plugging and abandonment that mitigates potential groundwater contamination.

As discussed earlier in this report, the reservoirs linked to these hot springs at depth have not been explored and thus the location of infrastructure necessary for exploration and development cannot be precisely constrained in this study. Although the specific details relative to critical habitat for threatened and/or endangered species cannot be directly addressed for any geothermal area in WPC as part of this study, the ability to customize the infrastructure layout at each geothermal area makes it possible to avoid conflicts with critical environmental habitat. In particular, deviated well-path technology allows great flexibility in well pad locations and ultimately road, pipeline, power plant, and power lines. The cumulative footprint for all parts of the infrastructure for a geothermal power plant is relatively small (figures 11, 12).



**Figure 12.** Photo of the 13.4 MWe capacity binary power plant at the Salt Wells geothermal area (figure 11). *Photo by Nicholas Hinz, 2011.*

# REPRESENTATIVE PROJECT DESCRIPTION/SCENARIO

The geothermal system at Monte Neva Hot Springs provides an example of possible multi-stage renewable energy development. Monte Neva Hot Springs is one of the four most promising known resources in WPC, which also include Williams hot springs, Cherry Creek Hot Springs, and the deep sedimentary resource in Steptoe Valley east of Cherry Creek Hot Springs. All four of these areas are located within 15 km of the new Southwest Intertie power line.

After an initial detailed review of existing data to determine the extent of past exploration activities, the first stages of exploration could focus on the development of a 5 to 20 MWe power plant that would harvest fluids from a moderate to shallow (1–2 km) reservoir, where fault-controlled convection has drawn higher-temperature fluids from depth. The knowledge learned during the development of this resource could be used to guide deeper exploration for fault-controlled permeable zones within the postulated deep carbonate stratigraphic aquifer at temperatures approaching 200°C and depths of 3–4 km. In this manner, development of the deep aquifer could begin by targeting the highest permeability zones intersected by young faults. In parallel with the development of electricity-grade resources, the surface hot springs at Monte Neva could be developed to support greenhouses or aquaculture. The relatively high spring temperatures (79°C) combined with high flow rates (625 gpm, Garside and Schilling, 1979) represent a significant heat flux well-suited for direct use heating of multiple buildings and greenhouses.

Previous geothermal exploration by Hunt Energy Corporation in Steptoe Valley focused on an area approximately 10 km north of Monte Neva Hot Springs. Drilling by Hunt encountered only conductive temperature gradients, but at Monte Neva Hot Springs, a maximum temperature of 88°C encountered in a shallow well (122 m depth) drilled by Magma Power Corp. in 1965 (Garside and Schilling, 1979) is significantly higher than predicted by the conductive gradients found by Hunt, requiring the presence of a significant component of fluid convection from depth. The K-Mg and Mg-corrected K-Na-Ca geothermometers predict subsurface temperatures of 46 and 40°C, respectively, which are much lower than the measured temperatures. These discrepancies, in combination with the relatively high Mg concentration of the spring water (21 mg/l), suggest that rising thermal fluids may be mixing with shallow, cooler groundwater. The rising thermal fluids could, therefore, have substantially higher temperatures before mixing, in turn indicating a more significant component of vertical convection. Additional geochemical analyses of nearby cold water chemistry could address the potential for mixing, and additional silica geothermometry data could also provide a valuable comparison for the cation geothermometry currently available.

## ACKNOWLEDGMENTS

Funding for this work was provided by a grant from the Department of Energy, Agreement Number DE-EE0003139, awarded to BEC Environmental, Inc., and provided to NBMG at UNR as a subcontract award. Thoughtful and detailed reviews were provided by Patrick Walsh and Mike Ressel. We thank Brenda Gilbert of BEC Environmental, Inc., and Jim Garza of White Pine County for the opportunity to contribute to this project and publish this report. This work was based on data available in 2013.

## REFERENCES

- Allis, R., Blackett, B., Gwynn, M., Hardwick, C., Moore, J., Morgan, C., Schelling, D., and Sprinkel, D.A., 2012, Stratigraphic reservoirs in the Great Basin—the bridge to development of enhanced geothermal systems in the US: Geothermal Resources Council Transactions, v. 36, p. 351–357.
- Allis, R., Moore, J., Gwynn, M., Kirby, S., and Sprinkel, D., 2011, The potential for basin-centered geothermal resources in the Great Basin: Geothermal Resources Council Transactions, v. 35, p. 683–688.
- Allis, R., Moore, J.N., Anderson, T., Deo, M., Kirby, S., Roehner, R., and Spencer, T., 2013, Characterizing the power potential of hot stratigraphic reservoirs in the western U.S.: Proceedings, 38<sup>th</sup> Workshop on Geothermal Reservoir Engineering, Stanford University, Stanford, CA, Feb. 11–13, 2013.
- Anderson, R.B., and Faulds, J.E., 2013, Structural controls of the Emerson Pass geothermal system, Washoe County, Nevada: Geothermal Resources Council Transactions, v. 37, p. 453–458.
- Anderson, T.C., 2013, Geothermal potential of deep sedimentary basins in the United States: Geothermal Resources Council Transactions, v. 37, p. 223–229.
- Barton, C. A., M. D. Zoback, and D. Moos, 1995, Fluid flow along potentially active faults in crystalline rock: Geology, v. 23, p. 683–686.
- Bell, J.W., and Ramelli, A.R., 2007, Active faults and neotectonics at geothermal sites in the western Basin and Range— preliminary results: Geothermal Resources Council Transactions, v. 31, p. 375–378.

- Coolbaugh, M., Zehner, R., Kreemer, C., Blackwell, D., Oppliger, G., Sawatzky, D., Blewitt, G., Pancha, A., Richards, M., Helm-Clark, C., Shevenell, L., Raines, G., Johnson, G., Minor, T., and Boyd, T., 2005, Geothermal potential map of the Great Basin, western United States: Nevada Bureau of Mines and Geology Map 151.
- Coolbaugh, M.F., Sladek, C., Kratt, C., Shevenell, L., and Faulds, J.E., 2006, Surface indicators of geothermal activity at Salt Wells, Nevada, USA, including warm ground, borate deposits, and siliceous alteration: *Geothermal Resources Council Transactions*, v. 30, p. 399–405.
- Crawford, I., 2013, This just in... Late breaking news from the global geothermal community: *Geothermal Resources Council Bulletin*, v. 42, no. 6, p. 46–49.
- Deo, M., Roehner, R., Allis, R., and Moore, J., 2013, Modeling of geothermal energy production from stratigraphic reservoirs in the Great Basin: *Geothermics*, v. 51, p. 38–45.
- Dominco, E. and Samilgil, E., 1970, The geochemistry of the Kizildere geothermal field, in the framework of the Saraykoy-Denizli geothermal area: *Geothermics*, special issue 2, v. 2, part 1, p. 553–560.
- Faulds, J.E., Hinz, N.H., Coolbaugh, M.F., Cashman, P.H., Kratt, C., Dering, G., Edwards, J., Mayhew, B., and McLachlan, H., 2011, Assessment of favorable structural settings of geothermal systems in the Great Basin, Western U.S.A.: *Geothermal Resources Council Transactions*, v. 35, p. 777–784.
- Faulds, J.E., Hinz, N.H., Dering, G.M., and Siler, D.L., 2013, The hybrid model—The most accommodating structural setting for geothermal power generation in the Great Basin, western U.S.A.: *Geothermal Resources Council Transactions*, v. 37, p. 3–10.
- Faulds, J.E., Hinz, N.H., Kreemer, C., and Coolbaugh, M., 2012, Regional patterns of geothermal activity in the Great Basin region, western U.S.A.—correlation with strain rates: *Geothermal Resources Council Transactions*, v. 36, p. 897–902.
- Ferrill, D.A., Winterle, J., Wittmeyer, G., Sims, D., Colton, S. and Armstrong, A., 1999, Stressed rock strains groundwater at Yucca Mountain, Nevada: *GSA Today*, v. 9, no. 5, p. 1–8.
- Garside, L.J. and Schilling, J.H., 1979, Thermal waters of Nevada: Nevada Bureau of Mines and Geology Bulletin 91, 163 p.
- Giggenbach, W.F., 1988, Geothermal solute equilibria—derivation of Na-K-Mg-Ca geoindicators: *Geochimica et Cosmochimica Acta*, v. 52, p. 2749–2765.
- Heidbach, O., Tingay, M., Barth, A., Reinecker, J., Kurfe, D. and Müller, B., 2008, The World Stress Map database release 2008 doi:10.1594/GFZ WSM Rel2008.
- Hinz, N.H., Faulds, J.E., and Bell, J.W., 2011, Preliminary geologic map of the Bunejug Mountains quadrangle, Churchill County, Nevada: Nevada Bureau of Mines and Geology Open-File Report 11-9, 1:24,000 scale, 1 sheet.
- Hinz, N.H., Faulds, J.E., and Coolbaugh, M.F., 2014, Association of fault terminations with fluid flow in the Salt Wells geothermal field, Nevada, U.S.A.: *Geothermal Resources Council Transactions*, v. 38, p. 3–9.
- Hinz, N.H., Faulds, J.E., and Siler, D.L., 2013, Developing systematic workflow from field work to quantitative 3D modeling for successful exploration of structurally controlled geothermal systems: *Geothermal Resources Council Transactions*, v. 37, p. 275–280.
- Jachens, R.C., Moring, B.C., and Schruben, P.G., 1996, Thickness of Cenozoic deposits and the isostatic residual gravity over basement, Chapter 2, in Singer, D.A., editors, An analysis of Nevada’s metal-bearing mineral deposits: Nevada Bureau of Mines and Geology Open-File Report 96-2, p. 2-1–2-10.
- Kennedy, B.M., and van Soest, M.C., 2007, Flow of mantle fluids through the ductile lower crust: Helium isotope trends: *Science*, v. 318, issue 5855, p. 1433–1436.
- Kirby, S.M., 2012, Summary of compiled permeability with depth measurements for basin fill, igneous, carbonate, and siliciclastic rocks in the Great Basin and adjoining regions: Utah Geological Survey Open-File Report 602, 9 p.
- Kratt, C., Sladek, C., and Coolbaugh, M., 2010, Boom and bust with the latest 2m temperature surveys—Dead Horse Wells, Hawthorne Army Depot, Terraced Hills, and other areas in Nevada: *Geothermal Resources Council Transactions*, v. 34, p. 567–574.
- Mariner, R.H., Presser, T.S., and Evans, W.C., 1983, Geochemistry of active geothermal systems in the northern Basin and Range Province: *Geothermal Resources Council Special Report No. 13*, May, 1983, p. 95–119.
- Morris, A., Ferrill, D.A. and Henderson, D.B., 1996, Slip-tendency analysis and fault reactivation: *Geology*, v. 24, no. 3, p. 275–278.
- NBMG and GBCGE, 2012, Great Basin groundwater geochemical database: accessed 2013, <http://www.nbmg.unr.edu/Geothermal/GeochemDatabase.html>.
- Orenstein, R., and Delwiche, B., 2014, The Don A. Campbell geothermal project: *Geothermal Resources Council Transactions*, v. 38, p. 91–98.
- Reed, M.J., and Mariner, R.H., 2007, Geothermal calculations for geothermal assessment: *Geothermal Resources Council Transactions*, v. 31, p. 89–92.
- Sibson, R.H., 1994, Crustal stress, faulting and fluid flow: Geological Society, London Special Publication, v. 78, p. 69–84.
- SMU, 2008, SMU Nevada database: accessed 2013, <http://smu.edu/geothermal/georesou/08%20Data/Nevada08.xls>.
- SMU, 2011, Temperature-at-depth maps 2011 update: accessed 2013, <http://www.google.org/egs>.
- Stewart, J.H., 1998, Regional characteristics, tilt domains, and extensional history of the late Cenozoic Basin and Range Province, western North America, in Faulds, J.E., and Stewart, J.H., editors, Accommodation zones and transfer zones—the regional segmentation of the Basin and Range province: Geological Society of America Special Paper 323, p. 47–74.
- Stewart, J.H., and Carlson, J.E., 1978, Geologic map of Nevada: U.S. Geological Survey MF-930, 1:500,000 scale, 1 sheet.
- Townend, J., and Zoback, M.D., 2000, How faulting keeps the crust strong: *Geology*, v. 28, no. 5, p. 399–402.
- USGS and NBMG, 2006, Quaternary fault and fold database for the United States: accessed 2013, from USGS web site: <http://earthquake.usgs.gov/hazards/qfaults/>.
- White, D.E., 1963, Preliminary evaluation of geothermal areas by geochemistry, geology, and shallow drilling: Proceedings U.N. Conference on New Sources of Energy: Solar Energy, Wind Power and Geothermal Energy, Rome, August 21–31, 1961, v. 2, p. 402–408.



White, D.E., 1968, Personal communication, U.S. Geological Survey, Menlo Park, by way of GEOTHERM Geochemical Database—U.S. Geological Survey: as contained Great Basin Groundwater Geochemical Database, University of Nevada, Reno, Nevada: <http://www.nbmgs.unr.edu/Geothermal/GeochemDatabase.html>.

***Suggested citation:***

Hinz, N.H., Coolbaugh, M.F., and Faulds, J.E., 2015, Geothermal resource potential assessment, White Pine County, Nevada: Nevada Bureau of Mines and Geology Report 55, 21 p.